Article

Using the InVEST-PLUS Model to Predict and Analyze the Pattern of Ecosystem Carbon storage in Liaoning Province, China

Pengcheng Li [1], Jundian Chen [2], Yixin Li [2] and Wen Wu [1,*]

1   JangHo Architecture College, Liaoning Provincial Key Laboratory of Urban and Architectural Digital Technology, Northeastern University, Shenyang 110819, China; 2201502@stu.neu.edu.cn
2   Geophysical Measuring Exploration Institute of Liaoning Province, Shenyang 110031, China; 13889317713@163.com (J.C.); kechuang1706@163.com (Y.L.)
*   Correspondence: wuwen@mail.neu.edu.cn

Abstract: Studying the spatiotemporal distribution pattern of carbon storage, balancing land development and utilization with ecological protection, and promoting urban low-carbon sustainable development are important topics under China's "dual carbon strategy" (Carbon emissions stabilize and harmonize with natural carbon absorption). However, existing research has paid little attention to the impact of land use changes under different spatial policies on the provincial-scale ecosystem carbon storage. In this study, we established a carbon density database for Liaoning Province and obtained the spatial and temporal distribution of carbon storage over the past 20 years. Then, based on 16 driving factors and multiple spatial policies in Liaoning Province, we predicted land use and land cover changes (LUCC) under three scenarios for 2050 and analyzed the spatiotemporal distribution characteristics and response mechanisms of carbon storage under different scenarios. The results showed that (1) LUCC directly affected carbon storage, with a 35.61% increase in construction land and a decrease in carbon storage of 0.51 Tg over the 20-year period. (2) From 2020 to 2050, the carbon storage varied significantly among the natural trend scenario (NTS), ecological restoration scenario (ERS), and economic priority scenario (EPS), with values of 2112.05 Tg, 2164.40 Tg, and 2105.90 Tg, respectively. Carbon storage in the ecological restoration scenario exhibited positive growth, mainly due to a substantial increase in forest area. (3) The spatial pattern of carbon storage in Liaoning Province was characterized by "low in the center, high in the east, and balanced in the west". Therefore, Liaoning Province can consider rationally formulating and strictly implementing the spatial policy of ecological protection in the future land planning so as to control the disorderly growth of construction land, realize the growth of ecological land area, effectively enhance carbon storage, and ensure the realization of the goal of "dual carbon strategy".

Keywords: carbon storage; land use change; multisource remote sensing data; InVEST model; PLUS model; Liaoning Province

1. Introduction

Global warming caused by greenhouse gas emissions such as carbon dioxide has become a serious climate problem facing human society and has a profound impact on global ecosystems [1]. In 2021, countries successively put forward the goal of achieving "net-zero carbon emissions" (Carbon emissions and the amount of natural removal to be balanced) [2]. The increase in terrestrial ecosystem carbon storage plays a vital role in reducing CO_2 content. LUCC directly cause changes in vegetation biomass and soil carbon sequestration, thus affecting carbon storage [3]. Carbon storage is widely considered to be a key indicator to measure the value of ecosystem services. By studying the response relationship and spatial distribution characteristics between carbon storage and LUCC, we can effectively monitor regional carbon changes [4].

At present, the evaluation methods of the LUCC response mechanism to carbon storage mainly include remote sensing estimation methods [5], empirical statistical models [6], and IPCC inventory approach [7,8]. Among them, the InVEST model can efficiently calculate and visualize carbon storage based on carbon pool data and has obvious advantages in reflecting the scale characteristics of carbon storage and the changes in spatiotemporal series [9]. At present, scholars from many countries have used the InVEST model to couple LUCC simulation models, such as CA-Markov, CLUE-S, SLEUTH, FLUS, revealing the spatiotemporal variation characteristics of carbon storage. Among the above models, the PLUS can best mine the inducement of various LUCC and simulate the patch-level changes. The model allows for the addition of future spatial policy elements, which can more scientifically simulate future LUCC under different policy scenarios [10,11]. Previous research has explored the influence of LUCC on carbon storage, including national [12], provincial [13], urban agglomeration [14,15], arid area [16], watershed [17,18], coastal zone [19], city [20,21], and county [22] scales. In summary, the existing research has extensively discussed the influence of LUCC on carbon storage and predicted future changes in carbon storage. However, most of these previous studies did not consider the impact of spatial planning policies on LUCC and carbon storage changes. Moreover, most of the previous prediction models lack the ability to mine LUCC-driving factors, resulting in a lack of reports on the linkage mechanism of LUCC-driving factors to carbon storage distribution.

Following the analysis of carbon storage by the InVEST model, scholars from various countries found that carbon storage and carbon density have generally shown a downward trend, and urbanization, farmland expansion, and deforestation were the main reasons [23,24]. However, some studies have found that ecological protection policies have greatly increased the coverage area of forests and grasslands, effectively inhibited the downward trend of carbon storage, and even increased carbon storage [25,26]. Therefore, to explore the effect of spatial planning policies, some scholars have carried out multi-scenario simulations of LUCC. Most of the research results show that the value of ecological service systems under ecological protection scenarios is significantly better than that under other scenarios (such as farmland protection scenarios and high urbanization scenarios) [27–29]. The spatial heterogeneity of carbon storage is often caused by many factors. Some studies have found that carbon storage-intensive areas are usually distributed in mountainous forest areas with higher altitudes. However, after the altitude exceeds 4000 m, the climate leads to a decline in biodiversity, and carbon storage decreases with increasing altitude [30,31]. Existing research on the driving factors shows that geographical factors (such as topography and slope) and climatic factors (such as annual average rainfall) are usually the main driving factors affecting carbon storage [32], and economic development sometimes promotes an increase in carbon storage [33].
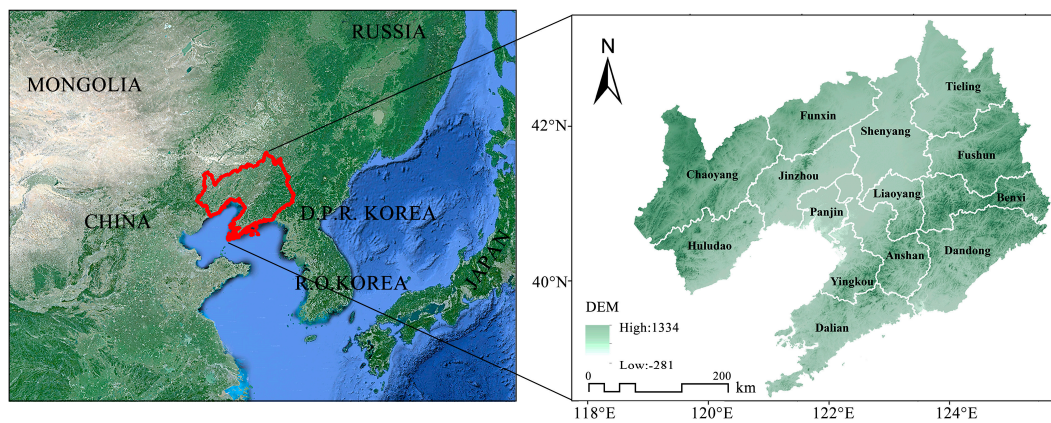
Liaoning Province, as China's heavy industrial base and a province with high energy consumption, is the key area to implement the dual carbon target. The Implementation Plan of Carbon Peak in Liaoning Province, promulgated in 2022, clearly pointed out the need to consolidate and enhance carbon sink capacity. This study estimates and predicts the carbon storage and its spatial pattern characteristics in Liaoning Province from 2000 to 2020 and in the future up to 2050 by using the InVEST and PLUS models. The purposes are as follows: (1) to elucidate the impact mechanism of the spatiotemporal evolution of LUCC on carbon storage in Liaoning Province in the last 20 years; (2) to study the impact of LUCC on carbon storage at provincial scale under the influence of different spatial policies in the future; and (3) to analyze the spatiotemporal distribution characteristics of carbon storage.

2. Materials and Methods

2.1. Study Area

Liaoning Province (E118°53′~125°46′, N38°45′~43°26′) is located in southern northeast China (Figure 1). The total area of Liaoning Province is 1.48×10^5 km^2. In 2020, the resident population was 42,591,407, and the regional GDP was 2758.41 billion yuan,

of which secondary industry accounted for 37.4%. Mountains and plains are the main geomorphological types in Liaoning Province, accounting for 59.5% and 32.4% of the area, respectively. Liaoning Province, as a critical heavy industrial base, has abundant natural resources and a solid industrial foundation and has made a tremendous contribution to the process of industrialization in China. In 2003, with the proposal of the "Revitalization Plan of Northeast China", Liaoning Province ushered in a new development peak. Energy-intensive industries such as equipment manufacturing, petrochemical, and metallurgical industries are the main economic pillars of Liaoning Province. In 2019, Liaoning Province emitted 533.4 Mt of carbon dioxide, accounting for 5.44% of the total emissions from China [34].

Figure 1. Location and terrain of Liaoning Province.

2.2. Methods

2.2.1. InVEST Model

The carbon storage module of the InVEST model assesses carbon storage using land use types as the units of measurement for the land surface. It can effectively evaluate the quantity and value of ecosystem services. The total carbon storage in the study area was estimated by multiplying the total area of different land types with their corresponding average carbon densities. We utilized the InVEST model to analyze carbon storage in Liaoning Province and predict its spatial distribution based on simulated LUCC in the province by 2050. The formulae are as follows:

$$C_i = C_{i\_above} + C_{i\_below} + C_{i\_soil} + C_{i\_dead} \tag{1}$$

$$C_{total} = \sum_{i=1}^{n} C_i \times S_i, \tag{2}$$

where i is the i-th land use type; C_i is the total carbon density of land use type i (Mg·hm^{-2}); C_{i_above}, C_{i_below}, C_{i_soil} and C_{i_dead} are the aboveground, underground, soil, and dead organic average carbon density of land use type i (Mg·hm^{-2}), respectively; C_{total} is the total carbon storage (Mg); S_i is the area of land use type i (hm^2); and n is the number of land use types, with a value of 6 in this study [35].

2.2.2. Markov-PLUS Model

The Markov model is a predictive method based on the Markov stochastic process. It utilizes an initial state vector and transfer probability matrix to forecast the future trend of LUCC change. This model is particularly suitable when landscape changes are not explicitly defined and exhibit a stable pattern. The calculation can be summarized as follows:

$$S_{t+1} = P_{mn} \times S_t, \tag{3}$$

where S_t is the land use situation in the period of t; S_{t+1} is the land use situation in the period of $t + 1$; and P_{mn} is the probability of land transfer from land use type m to land use type n.

In this study, we employ the Markov model to predict the land use demand for various types of land in Liaoning Province up to the year 2050, considering the change trend observed in the overall land use structure from 2010 to 2020. However, it is important to note that the Markov model alone does not account for the spatial variation of land types. To address this limitation, we complement our analysis by incorporating the PLUS model, which allows us to simulate the spatial evolution of land changes based on the predicted land demand.

PLUS is an LUCC model developed by Liang Xun et al. (2021) of China University of Geosciences. It has higher simulation accuracy and maneuverability than other models [36]. It integrates the stochastic seed mechanism in the planning development zone based on stochastic forest and takes the driving and guiding role of the ecological construction zone and planning development zone into account in the process of regional development. It is mainly based on LEAS and CARS. The LEAS module can sample the LUCC and use the stochastic forest algorithm to calculate the expansion odds of various types of land and the contribution rate of driving factors. Then, based on the CARS module, combined with the pixel values of different land types and the domain weights, the future LUCC can be simulated and predicted. The domain weight is determined based on the proportion of the expanded area for each land use type from 2000 to 2020, relative to the total expansion area. To achieve the optimal simulation results, the weight values have been fine-tuned as follows: 0.320 for farmland, 0.238 for forestland, 0.090 for grassland, 0.046 for water, 0.305 for construction land, and 0.001 for unused land.

This study first extracted the LUCC in Liaoning Province from 2000 to 2020 by the LEAS module, simulated the LUCC in 2020 by combining the data of 16 driving factors. In order to test the applicability of the PLUS model to the study area, we compared the land use data of Liaoning Province in 2020 simulated by the PLUS model with the real land use data of Liaoning Province in 2020 and used the Kappa coefficient and the overall accuracy to quantitatively describe the simulation accuracy. Usually, a value of kappa index greater than 0.8 is statistically satisfactory [11,37,38]. The verification results show that the Kappa coefficient and the overall accuracy reach 0.829 and 89.30%, respectively, which proves that the simulation accuracy meets the requirements, and the PLUS model can truly reflect the rule of spatial variation of land use in Liaoning Province. Therefore, the PLUS model is applicable to the LUCC simulation in Liaoning Province and can be used for LUCC prediction in the study area in 2050.

2.2.3. Scenario Setting

Considering that the social and economic development and natural conditions of different study areas have their own characteristics, the simulation of future land use spatial changes needs to be combined with the actual situation of the study area for specific analysis [39]. Based on the various development planning and policy frameworks of Liaoning Province, this study adds several spatial policy elements in the land and space planning of Liaoning Province and uses scenario analysis to assume three development scenarios.

- NTS: Assuming that the demand for land use is not affected by subsequent policies, continue to maintain the existing trend evolution.
- ERS: According to the principles of multiple ecological protection planning in Liaoning Province, ecological restoration and comprehensive management are promoted. It is assumed that under the ecological restoration scenario, the construction goal of increasing forestland coverage by 0.5% every 5 years in the 14th Five-Year Forestry and Grassland Development Plan of Liaoning Province must be achieved. In the Markov model, the probability of forestland conversion to other land uses is reduced by 60%, and the policy of returning farmland to forest and grassland and desertification control is further promoted. The probability of transfer of farmland and unused land outside

the permanent basic farmland area (farmland designated by the government that needs protection and cannot be used for other purposes) to forestland and grassland is increased by 20%. Adding forest parks and ecological protection red lines (areas with special and important ecological functions designated by the government) as forestland construction areas, the priority of forestland expansion in this area is higher than that of other land types.

- EPS: It is assumed that the study area will be driven by economic development in the future, and the probability of conversion from other land to construction land will increase by 20%. In order to attract external production factors and promote the economic development of Liaoning Province, national economic development zones and provincial economic development zones are added as economic construction zones; the priority of construction land expansion in this area is higher than that of other land types.

2.2.4. Spatial Autocorrelation Analysis

The average carbon density of each county is calculated in ArcGIS, and Moran's I value is calculated based on the carbon density value to obtain the global autocorrelation results. The range of Moran's I values is [−1, 1]. If the value is greater than 0, it means that the observed values of attributes have positive spatial correlation. Finally, local autocorrelation results and LISA (local indicators of spatial association) clustering of cities and counties are obtained via Anselin Local Moran's I.

2.3. Data Sources

2.3.1. The Remote Sensing Dataset of LUCC

In this study, the dataset of LUCC in Liaoning Province was derived from the land cover data of China, released by Professor Yang Jie and Huang Xin's team of Wuhan University. The overall accuracy of the dataset is 79.31%, and there are 9 first-level categories [40]. Referring to the classification of land resources, the land use types in Liaoning Province were reclassified into 6 types, namely farmland, forestland, grassland, water, construction land and unused land. To reduce the computation and ensure the accuracy of LUCC simulation, the spatial resolution was resampled to 90 m.

2.3.2. Carbon Density Data

The carbon pool data mainly refer to the public dataset and previous literature. In order to minimize the error, the carbon density data obtained via the field sampling of various types of land in Liaoning Province and adjacent research areas are selected as much as possible, and the average value is calculated. For carbon density data with multiple data sources, average processing is also performed. Some carbon density datasets further classify land use types into secondary classes, such as forests (subdivided into broad-leaved forests, coniferous forests, and coniferous and broad-leaved mixed forests). We calculate the carbon density based on the weighted average of the proportion of secondary land types in the third land survey and statistical yearbook published by Liaoning Province. Finally, we obtain the carbon density values of the four carbon pools corresponding to different land use types in Liaoning Province (Table 1).

2.3.3. Driving Factors Data

Selection of driving factors: The driving factors of LUCC mainly included 2 socioeconomic data points, 7 accessibility data points, and 7 climate and environmental data points (Table 2). To meet the requirements of the model's operation, all factor resolutions were uniformly resampled to a 90 m resolution. To ensure the scientific validity of factor contribution calculations, a normalization treatment was applied, normalizing the value range of each factor to [0, 1].

Table 1. Carbon density database of Liaoning Province (Mg·hm^{-2}).

Land Use Type	C_{i_above}	C_{i_below}	C_{i_soil}	C_{i_dead}	C_{total}	Data Sources
Farmland	21.09	9.07	72.34	0	102.50	[41–45]
Forestland	86.12	46.08	105.62	2.15	239.97	[43–46]
Grassland	14.34	14.15	56.81	0.24	85.54	[43–45,47–51]
Water	6.94	6.88	42.35	0.76	56.94	[43–45,52]
Construction land	10.51	8.24	41.78	0.58	61.11	[41,43,45,53–55]
Unused land	9.14	11.74	21.50	0	42.38	[44,45]

Table 2. Information related to LUCC driving factor data.

Data Category	Data Name	Data Source	Data Accuracy
Socioeconomic data	Population	Open Spatial Demographic Data and Research (https://www.worldpop.org/, accessed on 25 August 2022)	100 m × 100 m
	Gross Domestic Product (GDP)	Global Change Research Data Publishing & Repository (http://www.geodoi.ac.cn, accessed on 31 August 2022)	1 km × 1 km
Accessibility data	Distance to the railway Distance to the highway Distance to the expressway Distance to the trunk road Distance to the secondary trunk road Distance to the bypass Distance to the city center	OpenStreetMap (https://www.openstreetmap.org/, accessed on 24 August 2022)	90 m × 90 m
Climate and environmental data	Soil type	National Qinghai-Tibet Plateau Scientific Data Center (http://data.tpdc.ac.cn/, accessed on 18 October 2022)	1 km × 1 km
	Distance to the river	Open Street Map (https://www.openstreetmap.org/, accessed on 25 August 2022)	90 m × 90 m
	Annual average temperature Average annual rainfall	WorldClim (https://worldclim.org/data/index.html, accessed on 7 September 2022)	490 m × 490 m
	Digital elevation model (DEM) Slope Aspect of slope	Geospatial Data Cloud (http://www.gscloud.cn, accessed on 22 August 2022)	30 m × 30 m

3. Results

3.1. Spatial Change in Land Use

From 2000 to 2020, the proportion of farmland area was always the highest, followed by that of forestland and construction land (Table 3). Construction land and forestland increased continuously, and water increased and then decreased greatly. Among all land use types, construction land had the largest increase, increasing by 4008.57 km^2 in the past 20 years, an increase of 35.61%; grassland decreased by 2440.00 km^2 and farmland decreased by 2380.07 km^2, among which, grassland decreased the most, with a total decrease of 28.32%.
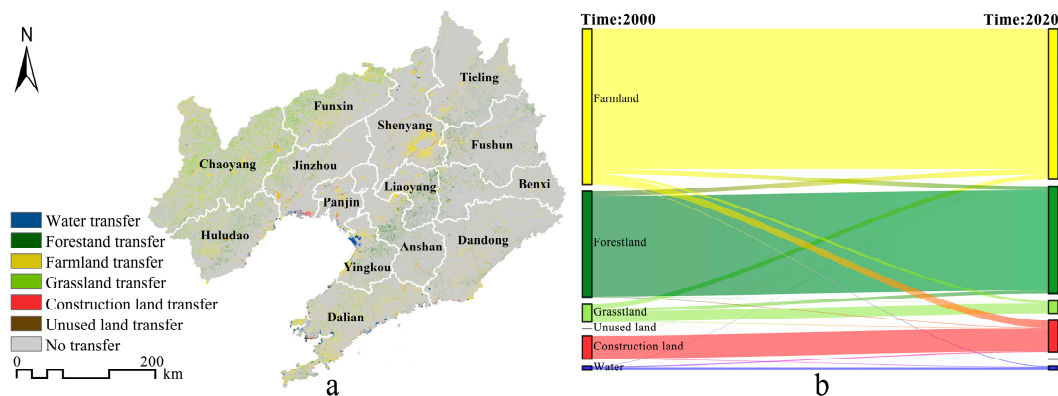
Table 3. LUCC area in different periods of Liaoning Province from 2000 to 2020 (km^2).

Land Use Type	2000	2010	2020	2000–2010	2010–2020	2000–2020
Farmland	73,575.60	72,171.92	71,195.53	−1403.68	−976.39	−2380.07
Forestland	50,445.49	50,873.41	51,297.33	427.92	423.92	851.84
Grassland	8616.00	7293.65	6176.00	−1322.35	−1117.65	−2440
Water	2059.21	2324.72	2053.03	265.51	−271.69	−6.18
Construction land	11,257.35	13,321.05	15,265.92	2063.70	1944.87	4008.57
Unused land	59.74	28.64	25.58	−31.10	−3.06	−34.16

From 2000 to 2020, the area of farmland transferred to construction land was the largest, reaching 3362.78 km^2, followed by the transfer of forestland and grassland to farmland, which had values of 2192.03 km^2 and 2072.93 km^2, respectively (Table 4). Figure 2a shows the spatial distribution of land use type transfer in Liaoning Province, and the main change patterns are visualized using a Sankey diagram in Figure 2b. The farmland with land type transfer was mainly distributed in the Shenyang modern metropolitan area, which means that Shenyang has developed outwards, occupying a large amount of farmland for urban construction. A large area of forestland was transferred to farmland and construction land in the eastern hilly zone, and the transfer area of forestland in the eastern hilly zone was more than that in the western zone.

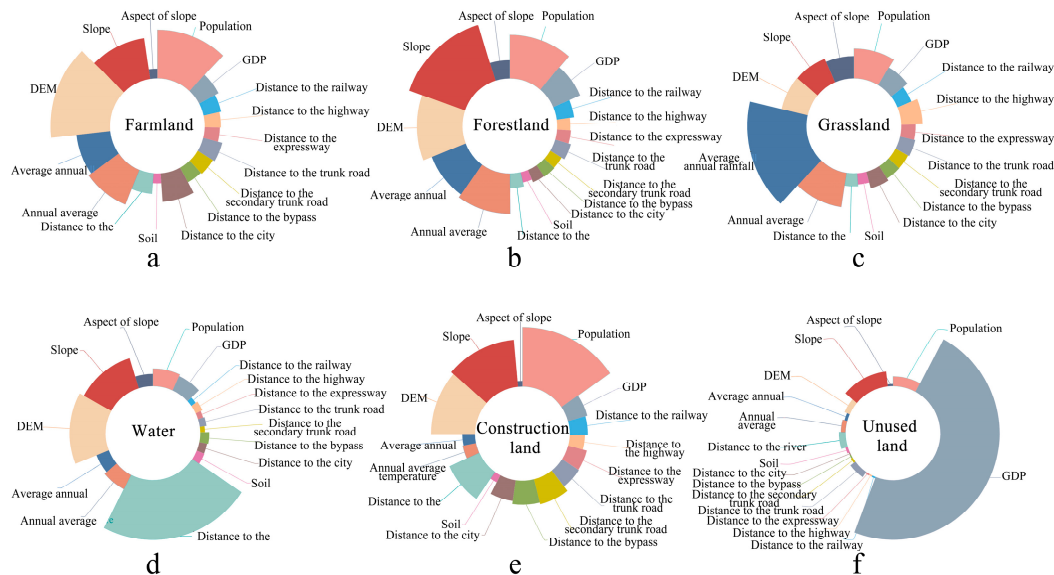**Table 4.** Transfer area of various land use types in Liaoning Province from 2000 to 2020 (km^2).

		2020						
		Farmland	Forestland	Grassland	Water	Construction Land	Unused Land	Total	Total Transfer-Out
	Farmland	66,679.63	1956.16	1177.92	396.37	3362.78	2.75	73,575.60	6895.98
	Forestland	2192.03	47,943.19	79.70	3.69	226.67	0.21	50,445.49	2502.30
	Grassland	2072.93	1391.73	4910.91	5.67	222.89	11.88	8616.00	3705.09
2000	Water	183.28	5.60	1.79	1407.20	458.00	3.35	2059.21	652.01
	Construction land	52.67	0.62	0.41	235.26	10,967.73	0.66	11,257.35	289.62
	Unused land	15.00	0.04	5.28	4.83	27.86	6.73	59.74	53.01
	Total	71,195.53	51,297.33	6176.00	2053.03	15,265.92	25.58	146,013.39	——
	Total transfer-in	4515.90	3354.15	1265.09	645.82	4298.19	18.85	——	14,098.00

Figure 2. (**a**) Areas where land use types have changed; (**b**) Sankey diagram of mutual conversion of different land use types.

3.2. Driving Forces of Land Use Change

According to Figure 3, population factors had a great impact on the changes in farmland, forestland, grassland, and construction land, with contribution rates of 0.119, 0.111, 0.086, and 0.154, respectively. The DEM, slope, and other topographic factors were the first three driving forces affecting the transformation of farmland, forestland, water, and construction land. The DEM factor was the largest driving force of farmland transformation, with a contribution rate of 0.143. The slope factor was the largest driving force of

forestland expansion, with a contribution rate of 0.148. The contribution rate of the GDP factor to unused land reached 0.480, which indicates that economic factors influence the development of unused land to a great extent.

Figure 3. Contribution rate of LUCC driving factors to the expansion of (**a**) farmland, (**b**) forestland, (**c**) grassland, (**d**) water, (**e**) construction land and (**f**) unused land.
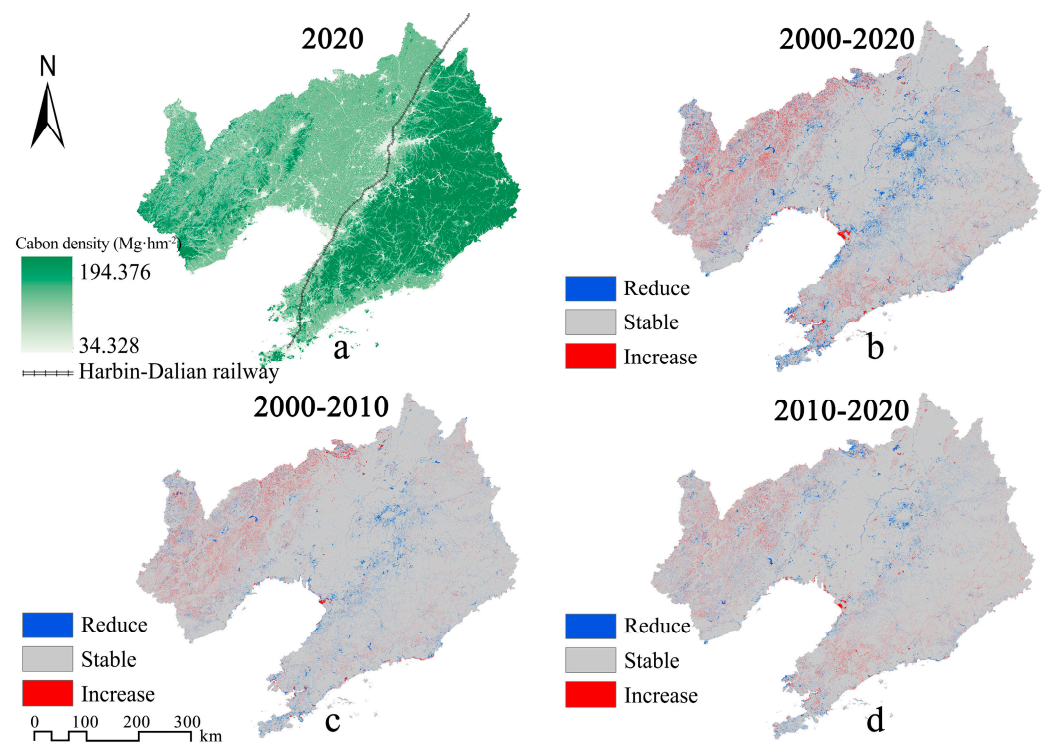
3.3. Spatiotemporal Variation Characteristics of Carbon Storage

The simulation results of carbon storage in Liaoning Province in 2000, 2010, and 2020 were 2119.16 Tg, 2117.72 Tg, and 2118.65 Tg, respectively. From 2000 to 2020, carbon storage decreased by approximately 0.51 Tg, and the average annual decrease was 0.03 Tg. In general, carbon storage showed a trend of decreasing first and then increasing slightly which decreased by 1.44 Tg from 2000 to 2010 and increased by 0.93 Tg from 2010 to 2020.

The distribution of carbon storage had significant spatial heterogeneity (Figure 4a), which is consistent with the topographic profile of "six mountains, one water, and three fields" in Liaoning Province. The northeastern low mountain area and the Liaodong Peninsula hilly area are divided by the Harbin-Dalian high-speed railway on the east side, and the western mountain and hilly area is composed of Nuluerhu Mountain, Songling Mountain, Heishan Mountain, and Yiwulu Mountain from northeast to southwest on the west side, constituting a high-density carbon storage area.

The increased areas of carbon storage in 2000–2020 were concentrated mainly in the hilly areas of western Liaoning and the reclamation area of the Yingkou Salt Field in Liaodong Bay (Figure 4b). From 2000 to 2010, the areas where carbon storage decreased significantly were mainly distributed in the periphery of Shenyang, Liaoyang, and Dalian and the coast of the Liaodong Peninsula (Figure 4c). After 2010, the growth of the urban construction land gradually slowed down, and the carbon storage reduction areas were scattered. From 2010 to 2020, only Shenyang was still expanding outward on a large scale, and the areas of carbon storage reduction were concentrated mainly in the periphery of Shenyang (Figure 4d).

Figure 4. (**a**) Spatial differentiation of carbon storage in Liaoning Province in 2020; (**b**–**d**) Change areas of carbon storage.
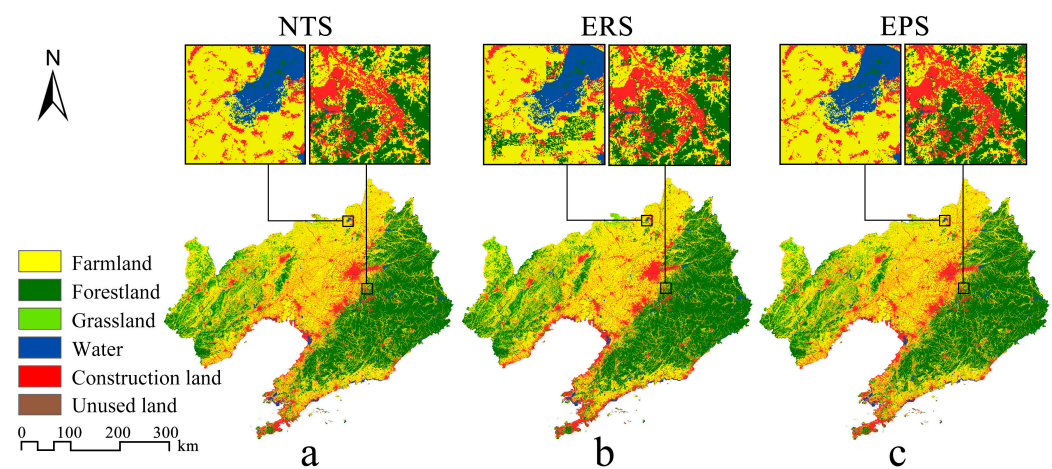
3.4. LUCC Simulation under Multiple Scenarios

Based on the PLUS model, the Markov model, and multiple policy constraints, the LUCC simulation of Liaoning Province in 2050 under NTS, ERS, and EPS was completed (Table 5). In 2050, the land use structure of the study area will still be dominated by forestland and farmland. Compared with 2020, the area of construction land under the three scenarios is increasing, which will increase by 3662.86 km^2, 3617.40 km^2, and 4903.59 km^2, respectively, with an increase of 23.99%, 23.70%, and 32.12%, respectively. Under the EPS, the increase in construction land is the largest, and the expansion of construction land is obvious. The main source of circulation is suburban farmland. The area of farmland under the three scenarios will shrink to varying degrees, which is expected to decrease by 3634.97 km^2, 7425.92 km^2, and 4526.16 km^2, respectively. Under the ERS, forestland will increase by 4349.30 km^2 compared with 2020, and forestland coverage will increase by 2.98%, basically completing the ecological restoration goal of increasing forestland coverage by 0.5% every 5 years. The forestland will increase by 549.20 km^2 and 444.61 km^2 under the NTS and the EPS, respectively. The growth of the forestland area under the ERS is significantly higher than other scenarios. In the next 30 years, the grassland area will be in a state of continuous reduction. Among them, the grassland under the EPS will decrease the most, which is 813.14 km^2. Under the ERS, the grassland area will change little, which is 538.92 km^2, because of the effective protection.

Table 5. Area of different land types under three scenarios in 2050 (km^2).

Land Use Type	2020	NTS	ERS	EPS
Farmland	71,195.53	67,560.56	63,769.61	66,669.37
Forestland	51,297.33	51,846.53	55,646.63	51,741.94
Grassland	6176.00	5606.36	5637.08	5362.86
Water	2053.03	2053.03	2057.08	2053.06
Construction land	15,265.92	18,928.78	18,883.32	20,169.51
Unused land	25.58	18.13	19.68	16.65

The land in the three scenarios presents a pattern of differentiated distribution in space. Under NTS, the spatial change of all kinds of land develops according to inertia, and the construction land increases are scattered (Figure 5a). Under the ERS, the growth of forestland is mainly in the areas with high ecological value such as the ecological red line and the surrounding areas of large area of water (Figure 5b). The source of forestland transfer is mainly the farmland area that needs to be returned to forest. At the same time, due to the limitation of permanent basic farmland policy under the ERS, the farmland in the Liaozhong plain area is protected, so the growth of construction land is mainly distributed in the coastal strip area that is not suitable for the growth of farmland and forestland. Under the EPS, the expansion of construction land is mainly concentrated in the economic development zone defined by the policy (Figure 5c) so as to maximize the contribution of construction land to economic growth.

Figure 5. LUCC in 2050 under (**a**) NTS, (**b**) ERS and (**c**) EPS.

3.5. Carbon Storage Estimation and Spatial Distribution Characteristics Analysis under Multiple Scenarios

3.5.1. Carbon Storage Estimation

In 2050, the carbon storage of Liaoning Province under NTS, ERS, and EPS is 2112.05 Tg, 2164.40 Tg, and 2105.90 Tg, respectively. Compared with 2020, the carbon storage will lose 6.60 Tg and 12.75 Tg under NTS and EPS, respectively, but the carbon storage will increase 45.75 Tg under ERS.
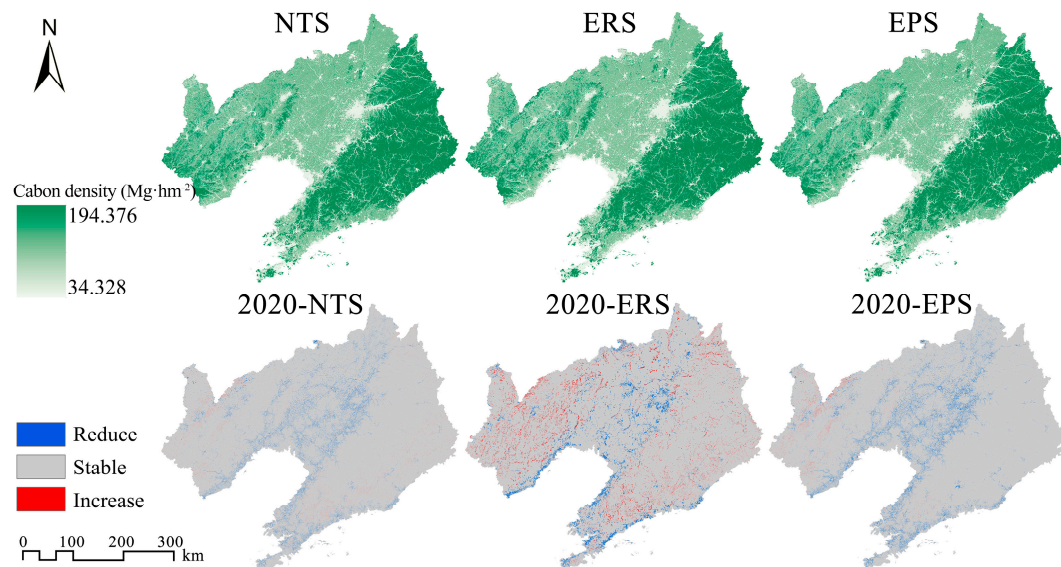
The response mechanisms of land transfer to carbon storage changes vary across the three scenarios (Table 6). In the NTS, the increased carbon storage will primarily result from the conversion of grassland and cropland to forestland, contributing an additional 4.72 Tg and 3.17 Tg, respectively. However, the conversion of farmland to construction land resulted in a loss of 13.62 Tg, leading to an overall decrease in carbon storage. In the ERS, a significant amount of grassland and cropland will be converted to forestland, increasing forest coverage, and adding a total of 58.37 Tg of carbon storage. This increase exceeds the carbon loss caused by the conversion of cropland to construction land, resulting in an overall growth in carbon storage. In the EPS, more cropland and grassland will be occupied by construction land for economic development, and the carbon storage loss from these conversions amounts to 18.73 Tg and 0.90 Tg, respectively.

Table 6. Carbon storage corresponding to land transfer under three scenarios from 2020 to 2050 (Tg).

	Carbon Storage Increase		Carbon Storage Reduce	
	Conversion of Major Land Use Types	Variation	Conversion of Major Land Use Types	Variation
NTS	Farmland–Forestland	4.72	Farmland–Construction land	−13.62
	Grassland–Forestland	3.17	Grassland–Construction land	−0.89
ERS	Farmland–Forestland	46.25	Farmland–Construction land	−16.52
	Grassland–Forestland	12.12	Farmland–Grassland	−0.37
EPS	Grassland–Forestland	6.86	Farmland–Construction land	−18.73
	Unused land–Construction land	0.01	Grassland–Construction land	−0.90

3.5.2. Spatial Pattern Prediction of Carbon Storage

In 2050, the carbon storage in Liaoning Province will be unevenly distributed (Figure 6). The areas with high carbon storage will still be concentrated mainly in the mountainous forest areas in western Liaoning and eastern Liaoning.

Figure 6. The spatial distribution and change areas of carbon storage under three scenarios.

In the NTS, the carbon storage reduction areas will be mainly in the core area of the development axis of the central Liaoning urban agglomeration.

In the ERS, in order to ensure the integrity of ecological land patches, the land tends to adopt an intensive development pattern. The regions with decreased carbon storage will be concentrated in the outskirts of major cities and along the Bohai Sea coast. On the other hand, the regions with increased carbon storage will be located within the western hilly areas of Liaoning Province and the Changbai Mountain range in the eastern part of Liaoning.
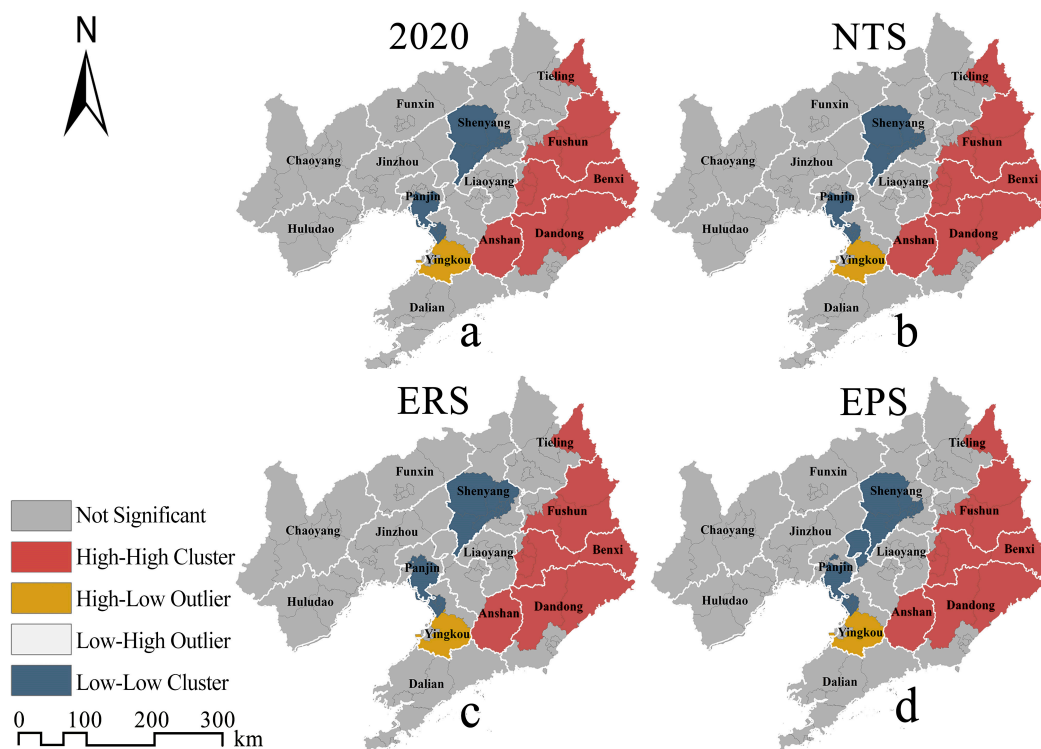
In the EPS, the carbon storage in the Liaoning central plain will significantly decrease. Due to the expansion of construction land in the economic development zones, the reduction in carbon storage will be more prominent. Only a small portion of Chaoyang City in western Liaoning will experience an increase in carbon storage.

3.5.3. Spatiotemporal Distribution Characteristics of Carbon Storage

To uncover the spatial agglomeration characteristics of carbon storage in future administrative units in Liaoning Province, this study employed spatial autocorrelation analysis to analyze the average carbon density of each district and county in the study area under

three scenarios. The results revealed Moran indices of 0.594, 0.586, and 0.592 for the three scenarios, respectively (*p* < 0.001). These findings indicate a significant positive correlation between high carbon density regions and their geographical locations, suggesting the presence of an agglomeration effect.

The LISA clustering shows that the high–high cluster areas under the three scenarios show consistency, mainly distributed in Tieling, Fushun, Benxi, Dandong, and Anshan, where Changbai Mountain is located. Fushun, Benxi, and Dandong, with the largest forest coverage area, are the most important high–high agglomeration areas. The high–low cluster area of carbon density is located in Yingkou, southwest of the high–high agglomeration area, with a small area. The low–low cluster areas of carbon density under the NTS will mainly be concentrated in Shenyang and Panjin (Figure 7b), which is consistent with 2020 (Figure 7a). In contrast, the ERS increases Shenbei New District of Shenyang and Xinglongtai District of Panjin (Figure 7c), and the EPS increases Taian County of Anshan and Shuangtaizi District of Panjin (Figure 7d). Due to the constraints on the ecological and farmland areas under the ERS, the low carbon density agglomeration area will mainly increase in the urban area of the city rather than the surrounding counties, while the construction land under the EPS will be more inclined to the direction of the metropolitan area, and the low–low cluster areas of carbon density will form a zonal distribution trend from Shenyang to the coastal urban area.

Figure 7. LISA clustering of carbon density under (**a**) 2020, (**b**) NTS, (**c**) ERS and (**d**) EPS.
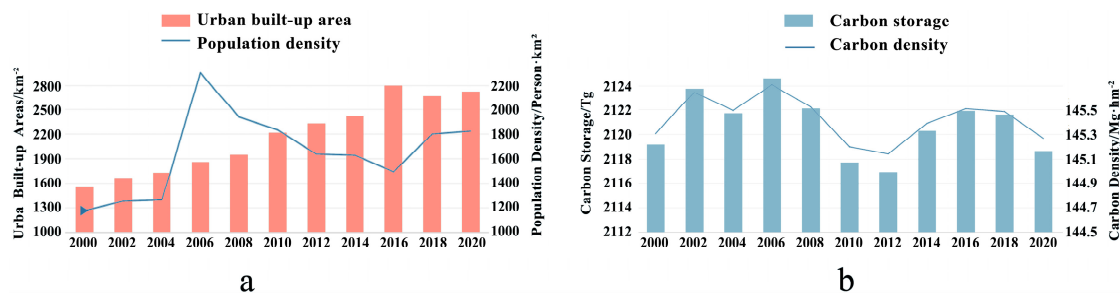
4. Discussion

4.1. Ecological and Development Problems Caused by Urbanization

Urban expansion brought by rapid urbanization will erode natural ecosystems such as green space ecosystems and farmland ecosystems, resulting in regional natural vegetation degradation and carbon storage reduction. According to the data of the China Statistical Yearbook (Figure 8a), Liaoning Province experienced large-scale urban expansion from 2000 to 2020, with the urban population density increasing by 630 person·km^{-2}, and the urban built-up area increasing from 1558.62 km^2 to 2725.60 km^2, an increase of 74.87%. Generally, LUCC in Liaoning Province is a process in which construction land encroaches on farmland, and farmland expands to consume forestland and grassland to ensure the development

of agriculture. From 2000 to 2020, the carbon storage in Liaoning Province showed a downward trend overall (Figure 8b). Similar conclusions can be found in other studies. Chen et al. (2019) found that the population and economy in the central part of Hunan Province in China have developed rapidly since the early 1960s, and that the original evergreen broad-leaved forest had been rapidly cut down and replaced by farmland, plantations, residential construction, or factories, thus resulting in low carbon storage [56]. Similarly, Sallustio et al. (2015) found that urbanization reduced carbon storage in the Molise region and the province of Rome (Italy) by approximately 0.25 Tg and 1.39 Tg, respectively, from 1990 to 2008 [57].

Figure 8. (**a**) Changes in population density and built-up area from 2000 to 2020; (**b**) carbon storage and carbon density change from 2000 to 2020.

Rapid urbanization not only brings ecological problems such as carbon storage decline but also brings economic development problems caused by non-intensive land development. The per capita construction land area in Liaoning Province has increased too quickly. As of 2015, 13 cities in Liaoning Province had exceeded the national standard (120 m^2). Li et al. (2020) showed that the growth of urban construction land in most cities in Liaoning Province leads to negative economic growth [58]. The inefficient use and extensive development mode of land development not only damages ecological security but also goes against the sound development of the regional economy. Therefore, urbanization needs a scientific strategy. Liaoning Province should reduce the dependence of urban economic growth on land, strictly control the large-scale expansion of cities, and pay attention to improving urbanization quality. We must eliminate the pattern of "grow first, clean up later", create sustainable cities, and coordinate ecological protection with economic development.

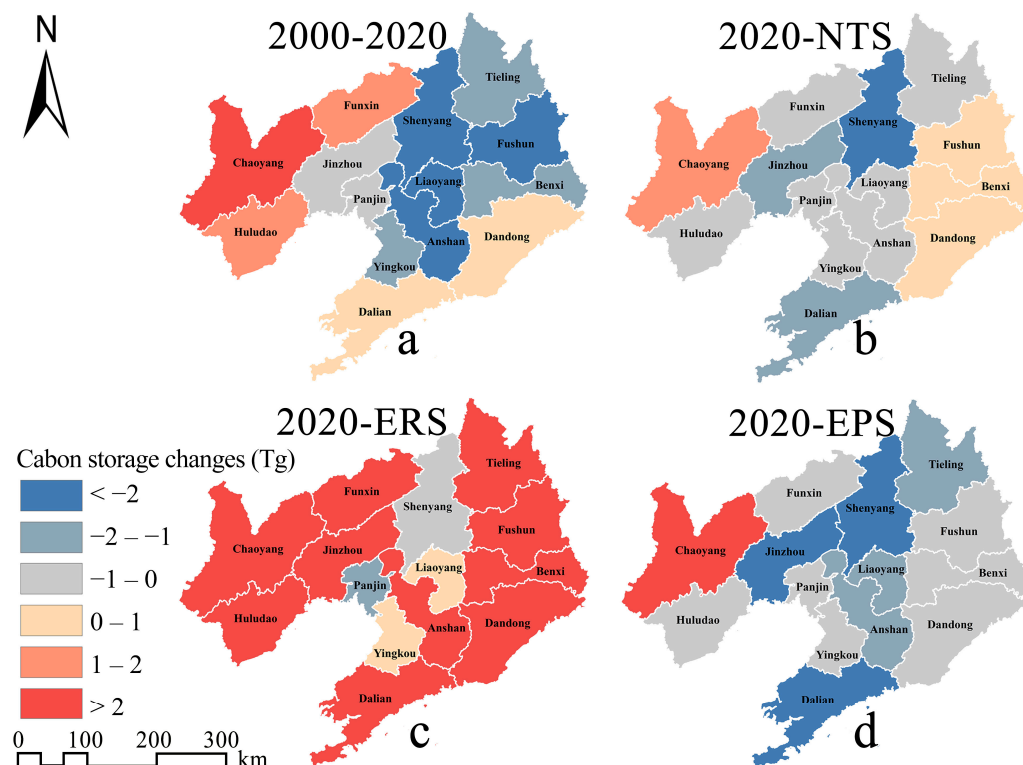### 4.2. Influence of LUCC Driving Factors on Carbon Storage

Human activity is the main driving force of LUCC, and LUCC is restricted by natural environmental factors and influenced by socioeconomic factors. The more frequent human activities are, the stronger the growth of urban construction land [59], the greater its impact on farmland, forestland, and grassland, and the greater its impact on the change in carbon storage. Among the driving factors, the population had a great influence on the changes in farmland, forestland, grassland, and construction land. This was mainly due to rapid urbanization accompanied by the growth of the urban population. Cities need to continuously expand their urban areas to accommodate and meet the needs of the growing population for living space, resulting in a decline in regional carbon density and carbon storage capacity.

The DEM factor was the largest driving force for the conversion of farmland, which may be because urban construction usually occurs in plain areas with low DEM values, resulting in the transfer of farmland to land with relatively high DEM values. Wang et al. (2022) analyzed the driving force of farmland growth in the Yangtze River Economic Belt and found that the DEM played a positive role in the early stage of farmland expansion. Over time, areas with a relatively high DEM that were suitable for farmland were used, and the DEM had a negative impact on farmland expansion at this time [60]. Therefore, the damage of farmland growth to carbon storage may decrease with the increase in altitude.

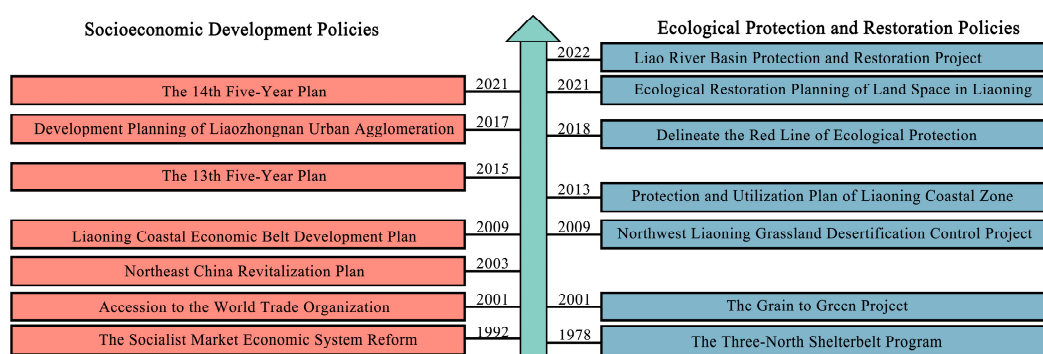### 4.3. Influence of Policy on Carbon Storage in Cities

Policies play a key role in promoting regional economic development and ecological restoration. Socioeconomic development policies may impose great pressure and challenges on the protection of ecosystems. Active ecological protection and restoration policies can effectively restore the stability and integrity of ecosystems and enhance regional carbon storage [61]. For example, Jerath et al. (2016) found that ecological policies affect the estimation of mangrove carbon storage in the Everglades of South Florida [62].

The carbon storage of all cities in the Liaohe Plain decreased from 2000 to 2020 (Figure 9a), among which the carbon storage in Liaoyang city, Shenyang city, Fushun city, and Anshan city all decreased by more than 2.00 Tg. According to the forecast, from 2020 to 2050, there will be 9 cities with decreased carbon storage in Liaoning Province under NTS (Figure 9b), while the number will reach 13 under EPS (Figure 9d).

Figure 9. Changes in carbon storage in cities of Liaoning Province from (**a**) 2000 to 2020, (**b**–**d**) 2020 to 2050 under NTS, ERS and EPS.

As shown in Figure 10, many development strategies, such as the Northeast China Revitalization Plan in 2003, had been implemented. China's 13th Five-Year Plan (2015–2020) vigorously supports the development of urban agglomerations in central and southern Liaoning. In the context of these policies, a large amount of investment in infrastructure and industrial construction has occurred, which has put great pressure on the management of ecosystems. Similar conclusions can be found in other studies. Li et al. (2017) found that government policies have greatly affected the rapid growth of artificial land cover in the coastal zone of Liaoning Province [63]. Mao et al. (2019) recorded the loss and degradation of large areas of wetlands and grasslands in Northeast China caused by policy drivers after 2000 [64].

Figure 10. Socioeconomic development policies and ecological protection and restoration policies implemented in Liaoning Province in recent 30 years.

From 2000 to 2020, the carbon storage of Chaoyang, Fuxin, and Huludao in the low hilly area of western Liaoning and Dalian and Dandong in the low hilly area of the Liaodong Peninsula increased. This was closely related to many forestry ecological projects, such as the Liaohe Shelterbelt System Construction Project, the Grain to Green Project, and the Grassland Desertification Control Project in Northwest Liaoning [65,66]. Liaoning Province strictly controlled the deforestation of natural forests and vigorously carried out afforestation campaigns supplemented by scientific forest management measures. The forestland landscape in western Liaoning has gradually changed from discrete small patches to connected large patches, the fragmentation degree has decreased, and the overall ecological function has increased, which reflects the strengthening of forest resource protection in Liaoning Province. From 2000 to 2020, the ecological policy achieved a net increase in forestland area of 851.84 km^2 in Liaoning Province, which was equivalent to an increase in carbon storage of 20.44 Tg. Previous studies have similar findings. For example, Muñoz-Rojas et al. (2011) found that afforestation and agricultural intensification policies increased the carbon storage of Andalusia (southern Spain) by 17.24 Tg from 1956 to 2007 [67]. In fact, compared with other provincial research areas in China, the absolute value of carbon storage reduction in Liaoning Province from 2000 to 2020 was relatively small, at 0.51 Tg. During the same period, Anhui Province lost 33.84 Tg [68], Guangdong Province lost 6.53 Tg [69], and Shandong Province lost 6.57 Tg [70]. The reason for these differences may be the effective implementation of ecological protection policies in Liaoning Province.

Under ERS, due to the effective implementation of the ecological protection red line and the policy of returning farmland to forest, the number of cities with increased carbon storage will increase to 12 (Figure 9c), which is three times that under NTS. Accordingly, it is important to formulate scientific ecological policies to protect and restore natural ecosystems to achieve sustainable ecosystem management and increase carbon storage.

4.4. Response Relationship between Land Use and Spatial Distribution of Carbon Storage

The spatial distribution of carbon storage was closely related to land use. The land development intensity in the central plain of Liaoning Province was high, and the land types were mainly farmland and construction land. The number of ecological patches such as forestland and grassland was small, and the degree of fragmentation was high, which does not provide high-density carbon storage space. Therefore, carbon storage is in a low agglomeration state in the central region. The topography and elevation of the hilly area of eastern Liaoning hinder the expansion of construction land and farmland to forestland, so the area maintains a high forest coverage and ecological integrity, which enables the region to have a significantly high carbon storage value. In general, the future spatial aggregation relationship of carbon storage has formed the structural characteristics of "low in the center, high in the east, and balanced in the west" in Liaoning Province.

4.5. Limitations

This study has reference value for optimizing the spatial layout of inter-provincial land and formulating low-carbon development strategies. However, there are still some limitations and uncertainties. (1) The InVEST model can efficiently calculate and visualize carbon storage based on carbon pool data. However, it assumes that the carbon density pool remains unchanged, which weakens the influence of environmental interference in the process of the carbon cycle and subsequent vegetation regeneration process [71]. The accuracy and real-time performance of parameters are common problems in this kind of research. These parameters can be verified by field sampling to reduce the potential uncertainty and obtain more reliable results. However, field sampling and surveys are expensive, and it is difficult to cover large and mesoscale study areas [72]. This study selected carbon density pools measured in the same study area and similar geographical location as much as possible to reduce the error of carbon storage evaluation. (2) The selection of spatial resolution is key to accurately simulating LUCC [73]. Based on previous studies [74], the resolution was resampled to 90 m to reduce the computation and improve the accuracy of the simulation. However, different study areas had different optimal simulation resolutions, so it is necessary to further study the best grid scale of LUCC simulation at the provincial scale.

5. Conclusions

This study discusses the spatial and temporal variation characteristics of carbon storage in Liaoning Province from 2000 to 2020 and predicts the change of carbon storage in 2050 under multiple scenarios. The results show that the construction land in Liaoning Province has increased significantly in the past 20 years, and the areas that reduce carbon storage are mainly distributed in the Liaohe Plain and the coastal economic belt of Liaoning Province. Driving factor analysis showed that the population, DEM, and slope were the main driving forces affecting the change in carbon storage.

In 2000, 2010, and 2020, the carbon storage in Liaoning Province was 2119.16 Tg, 2117.72 Tg, and 2118.65 Tg, respectively. Ecological policies effectively inhibited the decline in carbon storage. It is estimated that by 2050, the carbon storage in Liaoning Province under the NTS, ERS, and EPS will be 2112.05 Tg, 2164.40 Tg, and 2105.90 Tg, respectively, and the carbon storage under the ERS will achieve positive growth. There is significant spatial heterogeneity in the spatial distribution of carbon storage in Liaoning Province. The hilly area of the Liaodong Peninsula is a high-carbon-density area, while the highly developed central urban agglomeration and coastal economic belt urban agglomeration are low-carbon-density areas.

Liaoning Province, as a typical old industrial base, has had earlier urban construction and a higher degree of urbanization due to industrial expansion and resource development in the early stage of development. The development pattern of "grow first, clean up later" has brought about the decline in ecosystem service function. Cities should give full play to the advantages of their own regions according to different resources and socioeconomic conditions. In future development and construction, the ecological resources within the ecological protection red line should be strictly protected. At the same time, the development intensity of the Liaohe Plain and coastal land should be reasonably controlled to improve the intensive and economic ability of construction land. With the depletion of resources, industrial transformation, and system transitions, we should promote the transformation and revival of old industrial bases. It is necessary to explore the transformation from low-end industries to green industries and pay attention to ecological governance in order to achieve the goal of "carbon neutrality".

Conflicts of Interest: The authors declare no conflict of interest.

References

1. Cramer, W.; Guiot, J.; Fader, M.; Garrabou, J.; Gattuso, J.-P.; Iglesias, A.; Lange, M.A.; Lionello, P.; Llasat, M.C.; Paz, S.; et al. Climate change and interconnected risks to sustainable development in the Mediterranean. *Nat. Clim. Chang.* **2018**, *8*, 972–980. [CrossRef]
2. Sean, O.N. COP26: Some Progress, But Nations Still Fiddling While World Warms. *Engineering* **2022**, *11*, 6–8.
3. Chang, X.Q.; Xing, Y.Q.; Wang, J.Q.; Yang, H.; Gong, W.S. Effects of land use and cover change (LUCC) on terrestrial carbon stocks in China between 2000 and 2018. *Resour. Conserv. Recycl.* **2022**, *182*, 106333. [CrossRef]
4. He, C.Y.; Zhang, D.; Huang, Q.X.; Zhao, Y.Y. Assessing the potential impacts of urban expansion on regional carbon storage by linking the LUSD-urban and InVEST models. *Environ. Model. Softw.* **2016**, *75*, 44–58. [CrossRef]
5. Houghton, R.A.; Skole, D.L.; Lefkowitz, D.S. Changes in the landscape of Latin America between 1850 and 1985 II. Net release of CO2 to the atmosphere. *For. Ecol. Manag.* **1991**, *38*, 173–199. [CrossRef]
6. Zhuang, Q.W.; Shao, Z.F.; Gong, J.Y.; Li, D.R.; Huang, X.; Zhang, Y.; Xu, X.D.; Dang, C.Y.; Chen, J.L.; Altan, O.; et al. Modeling carbon storage in urban vegetation: Progress, challenges, and opportunities. *Int. J. Appl. Earth Obs. Geoinf.* **2022**, *114*, 103058. [CrossRef]
7. Mishra, U.; Torn, M.S.; Masanet, E.; Ogle, S.M. Improving regional soil carbon inventories: Combining the IPCC carbon inventory method with regression kriging. *Geoderma* **2012**, *189–190*, 288–295. [CrossRef]
8. Sperow, M. An enhanced method for using the IPCC approach to estimate soil organic carbon storage potential on U.S. agricultural soils. *Agric. Ecosyst. Environ.* **2014**, *193*, 96–107. [CrossRef]
9. He, Y.L.; Ma, J.M.; Zhang, C.S.; Yang, H. Spatio-Temporal Evolution and Prediction of Carbon Storage in Guilin Based on FLUS and InVEST Models. *Remote Sens.* **2023**, *15*, 1445. [CrossRef]
10. Wei, Q.Q.; Abudureheman, M.; Halike, A.; Yao, K.X.; Yao, L.; Tang, H.; Tuheti, B. Temporal and spatial variation analysis of habitat quality on the PLUS-InVEST model for Ebinur Lake Basin, China. *Ecol. Indic.* **2022**, *145*, 109632. [CrossRef]
11. Li, C.; Wu, Y.M.; Gao, B.P.; Zheng, K.J.; Wu, Y.; Li, C. Multi-scenario simulation of ecosystem service value for optimization of land use in the Sichuan-Yunnan ecological barrier, China. *Ecol. Indic.* **2021**, *132*, 108328. [CrossRef]
12. Lv, X.Y.; Qiao, Y.; Yu, J.Q.; Gong, S.Y.; Hao, L.L. Analysis and Prediction of Forest Carbon Storage and Carbon Sequestration Capacity in China. *Acad. J. Environ. Earth Sci.* **2022**, *4*, 25–30.
13. Tang, L.P.; Ke, X.L.; Zhou, T.; Zheng, W.W.; Wang, L.Y. Impacts of cropland expansion on carbon storage: A case study in Hubei, China. *J. Environ. Manag.* **2020**, *265*, 110515. [CrossRef] [PubMed]
14. Jiang, W.G.; Deng, Y.; Tang, Z.H.; Lei, X.; Chen, Z. Modelling the potential impacts of urban ecosystem changes on carbon storage under different scenarios by linking the CLUE-S and the InVEST models. *Ecol. Model.* **2017**, *345*, 30–40. [CrossRef]
15. Wu, W.H.; Xu, L.Y.; Zheng, H.Z.; Zhang, X.R. How much carbon storage will the ecological space leave in a rapid urbanization area? Scenario analysis from Beijing-Tianjin-Hebei Urban Agglomeration. *Resour. Conserv. Recycl.* **2023**, *189*, 106774. [CrossRef]
16. Zhu, G.F.; Qiu, D.D.; Zhang, Z.X.; Sang, L.Y.; Liu, Y.W.; Wang, L.; Zhao, K.L.; Ma, H.Y.; Xu, Y.X.; Wan, Q.Z. Land-use changes lead to a decrease in carbon storage in arid region, China. *Ecol. Indic.* **2021**, *127*, 107770. [CrossRef]
17. Gai, Z.X.; Xu, Y.; Du, G.M. Spatio-Temporal Differentiation and Driving Factors of Carbon Storage in Cultivated Land-Use Transition. *Sustainability* **2023**, *15*, 3897. [CrossRef]
18. Dida, J.J.; Tiburan, C.; Tsutsumida, N.; Saizen, I. Carbon Stock Estimation of Selected Watersheds in Laguna, Philippines Using InVEST. *Philipp. J. Sci.* **2021**, *150*, 501–513. [CrossRef]
19. Zhu, L.Y.; Song, R.X.; Sun, S.; Li, Y.; Hu, K. Land use/land cover change and its impact on ecosystem carbon storage in coastal areas of China from 1980 to 2050. *Ecol. Indic.* **2022**, *142*, 109178. [CrossRef]
20. Nie, X.; Lu, B.; Chen, Z.P.; Yang, Y.W.; Chen, S.; Chen, Z.H.; Wang, H. Increase or decrease? Integrating the CLUMondo and InVEST models to assess the impact of the implementation of the Major Function Oriented Zone planning on carbon storage. *Ecol. Indic.* **2020**, *118*, 106708. [CrossRef]
21. Li, L.; Song, Y.; Wei, X.H.; Dong, J. Exploring the impacts of urban growth on carbon storage under integrated spatial regulation: A case study of Wuhan, China. *Ecol. Indic.* **2020**, *111*, 106064. [CrossRef]
22. Wang, N.F.; Chen, X.P.; Zhang, Z.L.; Pang, J.X. Spatiotemporal dynamics and driving factors of county-level carbon storage in the Loess Plateau: A case study in Qingcheng County, China. *Ecol. Indic.* **2022**, *144*, 109460. [CrossRef]
23. Liu, X.P.; Wang, S.J.; Wu, P.J.; Feng, K.S.; Klaus, H.; Li, X.; Sun, L.X. Impacts of Urban Expansion on Terrestrial Carbon Storage in China. *Environ. Sci. Technol.* **2019**, *53*, 6834–6844. [CrossRef]
24. Clerici, N.; Cote-Navarro, F.; Escobedo, F.J.; Rubiano, K.; Villegas, J.C. Spatio-temporal and cumulative effects of land use-land cover and climate change on two ecosystem services in the Colombian Andes. *Sci. Total Environ.* **2019**, *685*, 1181–1192. [CrossRef]

25. Li, K.M.; Cao, J.J.; Adamowski, J.F.; Biswas, A.; Zhou, J.J.; Liu, Y.J.; Zhang, Y.K.; Liu, C.F.; Dong, X.G.; Qin, Y.L. Assessing the effects of ecological engineering on spatiotemporal dynamics of carbon storage from 2000 to 2016 in the Loess Plateau area using the InVEST model: A case study in Huining County, China. *Environ. Dev.* **2021**, *39*, 100641. [CrossRef]

26. Zhao, M.M.; He, Z.B.; Du, J.; Chen, L.F.; Lin, P.F.; Fang, S. Assessing the effects of ecological engineering on carbon storage by linking the CA-Markov and InVEST models. *Ecol. Indic.* **2019**, *98*, 29–38. [CrossRef]

27. Zhu, X.J.; Li, J.X.; Cheng, H.; Zheng, L.G.; Huang, W.S.; Yan, Y.; Liu, H.; Yang, X.Y. Assessing the impacts of ecological governance on carbon storage in an urban coal mining subsidence area. *Ecol. Inform.* **2022**, *72*, 101901. [CrossRef]

28. Lahiji, R.N.; Dinan, N.M.; Liaghati, H.; Ghaffarzadeh, H.; Vafaeinejad, A. Scenario-based estimation of catchment carbon storage: Linking multi-objective land allocation with InVEST model in a mixed agriculture-forest landscape. *Front. Earth Sci.* **2020**, *14*, 1–10. [CrossRef]

29. Xiang, S.J.; Wang, Y.; Deng, H.; Yang, C.M.; Wang, Z.F.; Gao, M. Response and multi-scenario prediction of carbon storage to land use/cover change in the main urban area of Chongqing, China. *Ecol. Indic.* **2022**, *142*, 109205. [CrossRef]

30. Zhang, Y.Q.; Ai, J.J.; Sun, Q.W.; Li, Z.C.; Hou, L.Y.; Song, L.G.; Tang, G.Y.; Li, L.; Shao, G.D. Soil organic carbon and total nitrogen stocks as affected by vegetation types and altitude across the mountainous regions in the Yunnan Province, south-western China. *Catena* **2021**, *196*, 104872. [CrossRef]

31. Duan, X.W.; Rong, L.; Hu, J.M.; Zhang, G.L. Soil organic carbon stocks in the Yunnan Plateau, southwest China: Spatial variations and environmental controls. *J. Soils Sediments* **2014**, *14*, 1643–1658. [CrossRef]

32. Aneseyee, A.B.; Soromessa, T.; Elias, E.; Noszczyk, T.; Hernik, J.; Benti, N.E. Expressing carbon storage in economic terms: The case of the upper Omo Gibe Basin in Ethiopia. *Sci. Total Environ.* **2022**, *808*, 152166. [CrossRef]

33. Wang, Z.; Zeng, J.; Chen, W.X. Impact of urban expansion on carbon storage under multi-scenario simulations in Wuhan, China. *Environ. Sci. Pollut. Res.* **2022**, *29*, 45507–45526. [CrossRef] [PubMed]

34. Li, Z.L.; Dai, H.C.; Sun, L.; Xie, Y.; Liu, Z.; Wang, P.; Yabar, H. Exploring the impacts of regional unbalanced carbon tax on CO_2 emissions and industrial competitiveness in Liaoning province of China. *Energy Policy* **2018**, *113*, 9–19. [CrossRef]

35. Shen, L.; Zeng, Q. Multiscenario simulation of land use and land cover in the Zhundong mining area, Xinjiang, China. *Ecol. Indic.* **2022**, *145*, 109608. [CrossRef]

36. Liang, X.; Guan, Q.F.; Clarke, K.C.; Liu, S.S.; Wang, B.Y.; Yao, Y. Understanding the drivers of sustainable land expansion using a patch-generating land use simulation (PLUS) model: A case study in Wuhan, China. *Comput. Environ. Urban Syst.* **2021**, *85*, 101569. [CrossRef]

37. Huang, D.; Huang, J.; Liu, T. Delimiting urban growth boundaries using the CLUE-S model with village administrative boundaries. *Land Use Policy* **2019**, *82*, 422–435. [CrossRef]

38. Lin, W.; Sun, Y.; Nijhuis, S.; Wang, Z. Scenario-based flood risk assessment for urbanizing deltas using future land-use simulation (FLUS): Guangzhou Metropolitan Area as a case study. *Sci. Total Environ.* **2020**, *739*, 139899. [CrossRef]

39. Gong, W.; Duan, X.; Sun, Y.; Zhang, Y.; Ji, P.; Tong, X.; Qiu, Z.; Liu, T. Multi-scenario simulation of land use/cover change and carbon storage assessment in Hainan coastal zone from perspective of free trade port construction. *J. Clean. Prod.* **2023**, *385*, 135630. [CrossRef]

40. Yang, J.; Huang, X. The 30 m annual land cover dataset and its dynamics in China from 1990 to 2019. *Earth Syst. Sci. Data* **2021**, *13*, 3907–3925. [CrossRef]

41. Mei, H.; Ji, J.J.; Cao, M.K.; Li, K.R. Modeling study of vegetation shoot and root biomass in China. *Acta Ecol. Sin.* **2006**, *26*, 4156–4163. (In Chinese)

42. Liu, H.Y. Dynamics Change and Quantification of Sequestration Potential for Soil Organic Carbon in Croplands in Liaoning Province. Ph.D. Thesis, Shenyang Agricultural University, Shenyang, China, 2011. (In Chinese).

43. Li, H.Y. The Evaluation on Ecological Effects of the Project of Returning Farmland to Forest in Liaoning Province, based on Remote Sensing and InVEST Model. Ph.D. Thesis, Jilin University, Changchun, China, 2019. (In Chinese).

44. Xu, L.; He, N.P.; Yu, G.R. A dataset of carbon density in Chinese terrestrial ecosystems (2010s). *Sci. Data Bank* **2019**, *4*, 90–96.

45. Spawn, S.A.; Sullivan, C.C.; Lark, T.J.; Gibbs, H.K. Harmonized global maps of above and belowground biomass carbon density in the year 2010. *Sci. Data* **2020**, *7*, 112. [CrossRef] [PubMed]

46. Wang, X.L.; Wang, T.; Lv, G. Spatial distribution of Forest Aboveground Biomass in Northeast China (2020). 2022. [CrossRef]

47. Ma, W.H.; Fang, J.Y.; Yang, Y.H.; Mohammat, A. Biomass carbon stocks and their changes in northern China's grasslands during 1982–2006. *Sci. China Life Sci.* **2010**, *53*, 841–850. [CrossRef]

48. Fan, J.W.; Zhong, H.P.; Harris, W.; Yu, G.R.; Wang, S.Q.; Hu, Z.M.; Yue, Y.Z. Carbon storage in the grasslands of China based on field measurements of above- and below-ground biomass. *Clim. Chang.* **2008**, *86*, 375–396. [CrossRef]

49. Wu, H.B.; Guo, Z.T.; Peng, C.H. Distribution and storage of soil organic carbon in China. *Glob. Biogeochem. Cycles* **2003**, *17*, 1–11. [CrossRef]

50. Ni, J. Forage Yield-Based Carbon Storage in Grasslands of China. *Clim. Chang.* **2004**, *67*, 237–246. [CrossRef]

51. Yang, Y.H.; Fang, J.Y.; Ma, W.H.; Smith, P.; Mohammat, A.; Wang, S.P.; Wang, W. Soil carbon stock and its changes in northern China's grasslands from 1980s to 2000s. *Glob. Chang. Biol.* **2010**, *16*, 3036–3047. [CrossRef]

52. LI, J.P.; XIA, S.X.; YU, X.B.; Li, X.S.; Xu, C.; Zhao, N.; Wang, S.T. Evaluation of Carbon Storage on Terrestrial Ecosystem in Hebei Province Based on InVEST Model. *J. Ecol. Rural. Environ.* **2020**, *36*, 854–861. (In Chinese)

53. Liu, C.F.; He, X.Y.; Chen, W.; Zhao, G.L. Analysis of environmental benefits of vegetation in Shenyang built-up areas. *Liaoning For. Sci. Technol.* **2006**, *2*, 1–3+31+55. (In Chinese)

54. Zhu, C.; Zhou, S.Q.; Zhou, D.C. Organic carbon storage in urban built-up areas of China in 1997–2006. *Chin. J. Appl. Ecol.* **2012**, *23*, 1195–1202. (In Chinese)

55. Wang, D.S. Studies on Net Carbon Reserves in Beijing Urban Landscape Green Based on Biomass Measurement. Ph.D. Thesis, Beijing Forestry University, Beijing, China, 2010. (In Chinese).

56. Chen, L.C.; Guan, X.; Li, H.M.; Wang, Q.K.; Zhang, W.D.; Yang, Q.P.; Wang, S.L. Spatiotemporal patterns of carbon storage in forest ecosystems in Hunan Province, China. *For. Ecol. Manag.* **2019**, *432*, 656–666. [CrossRef]

57. Sallustio, L.; Quatrini, V.; Geneletti, D.; Corona, P.; Marchetti, M. Assessing land take by urban development and its impact on carbon storage: Findings from two case studies in Italy. *Environ. Impact Assess. Rev.* **2015**, *54*, 80–90. [CrossRef]

58. Li, Z.Y.; Luan, W.X.; Zhang, Z.C.; Su, M. Relationship between urban construction land expansion and population/economic growth in Liaoning Province, China. *Land Use Policy* **2020**, *99*, 105022. [CrossRef]

59. Kuang, W.H.; Liu, J.Y.; Dong, J.W.; Chi, W.W.; Zhang, C. The rapid and massive urban and industrial land expansions in China between 1990 and 2010: A CLUD-based analysis of their trajectories, patterns, and drivers. *Landsc. Urban Plan.* **2016**, *145*, 21–33. [CrossRef]

60. Wang, L.Y.; Zhang, S.Y.; Xiong, Q.Q.; Liu, Y.; Liu, Y.F.; Liu, Y.L. Spatiotemporal dynamics of cropland expansion and its driving factors in the Yangtze River Economic Belt: A nuanced analysis at the county scale. *Land Use Policy* **2022**, *119*, 106168. [CrossRef]

61. Zhou, J.J.; Zhao, Y.R.; Huang, P.; Zhao, X.; Feng, W.; Li, Q.Q.; Xue, D.X.; Dou, J.; Shi, W.; Wei, W.; et al. Impacts of ecological restoration projects on the ecosystem carbon storage of inland river basin in arid area, China. *Ecol. Indic.* **2020**, *118*, 106803. [CrossRef]

62. Jerath, M.; Bhat, M.; Rivera-Monroy, V.H.; Castañeda-Moya, E.; Simard, M.; Twilley, R.R. The role of economic, policy, and ecological factors in estimating the value of carbon stocks in Everglades mangrove forests, South Florida, USA. *Environ. Sci. Policy* **2016**, *66*, 160–169. [CrossRef]

63. Li, H.Y.; Man, W.D.; Li, X.Y.; Ren, C.Y.; Wang, Z.M.; Li, L.; Jia, M.M.; Mao, D.H. Remote sensing investigation of anthropogenic land cover expansion in the low-elevation coastal zone of Liaoning Province, China. *Ocean. Coast. Manag.* **2017**, *148*, 245–259. [CrossRef]

64. Mao, D.H.; He, X.Y.; Wang, Z.M.; Tian, Y.L.; Xiang, H.X.; Yu, H.; Man, W.D.; Jia, M.M.; Ren, C.Y.; Zheng, H.F. Diverse policies leading to contrasting impacts on land cover and ecosystem services in Northeast China. *J. Clean. Prod.* **2019**, *240*, 117961. [CrossRef]

65. Chu, X.; Zhan, J.Y.; Li, Z.H.; Zhang, F.; Qi, W. Assessment on forest carbon sequestration in the Three-North Shelterbelt Program region, China. *J. Clean. Prod.* **2019**, *215*, 382–389. [CrossRef]

66. Li, H.Y.; Mao, D.H.; Li, X.Y.; Wang, Z.M.; Jia, M.M.; Huang, X.; Xiao, Y.H.; Xiang, H.X. Understanding the contrasting effects of policy-driven ecosystem conservation projects in northeastern China. *Ecol. Indic.* **2022**, *135*, 108578. [CrossRef]

67. Muñoz-Rojas, M.; De la Rosa, D.; Zavala, L.M.; Jordán, A.; Anaya-Romero, M. Changes in land cover and vegetation carbon stocks in Andalusia, Southern Spain (1956–2007). *Sci. Total Environ.* **2011**, *409*, 2796–2806. [CrossRef] [PubMed]

68. Yang, Q.Q.; Zhang, P.; Qiu, X.C.; Qiu, X.C.; Xu, G.L.; Xu, G.L.; Chi, J.Y. Spatial-Temporal Variations and Trade-Offs of Ecosystem Services in Anhui Province, China. *Int. J. Environ. Res. Public Health* **2023**, *20*, 855. [CrossRef]

69. Lin, T.; Yang, M.Z.; Liu, F.; Yang, H.J.; Wang, Y.J. Spatial correlation and prediction of land use carbon storage based on the InVEST-PLUS model- A case study in Guangdong Province. *China Environ. Sci.* **2022**, *42*, 4827–4839. (In Chinese)

70. Zhu, L.Y.; Xing, H.Q.; Hou, D.Y. Analysis of carbon emissions from land cover change during 2000 to 2020 in Shandong Province, China. *Sci. Rep.* **2022**, *12*, 8021. [CrossRef]

71. Qiu, Z.X.; Feng, Z.K.; Song, Y.N.; Li, M.L.; Zhang, P.P. Carbon sequestration potential of forest vegetation in China from 2003 to 2050: Predicting forest vegetation growth based on climate and the environment. *J. Clean. Prod.* **2020**, *252*, 119715. [CrossRef]

72. Hu, X.P.; Hou, Y.Z.; Li, D.; Hua, T.; Marchi, M.; Paola Forero Urrego, J.; Huang, B.; Zhao, W.W.; Cherubini, F. Changes in multiple ecosystem services and their influencing factors in Nordic countries. *Ecol. Indic.* **2023**, *146*, 109847. [CrossRef]

73. Díaz-Pacheco, J.; van Delden, H.; Hewitt, R. The Importance of Scale in Land Use Models: Experiments in Data Conversion, Data Resampling, Resolution and Neighborhood Extent. In *Geomatic Approaches for Modeling Land Change Scenarios*; Camacho Olmedo, M.T., Paegelow, M., Mas, J.-F., Escobar, F., Eds.; Springer International Publishing: Cham, Switzerland, 2018; pp. 163–186.

74. Samat, N. Characterizing the scale sensitivity of the cellular automata simulated urban growth: A case study of the Seberang Perai Region, Penang State, Malaysia. *Comput. Environ. Urban Syst.* **2006**, *30*, 905–920. [CrossRef]